Original Research

HPRUNET: A High-Precision Network for ALCAPA Segmentation with Residual Learning and Conditional Refinement

C. Rajeev[1*], Karthika Natarajan[2]

Received: 23 July 2025 / Accepted: 20 September 2025 / Published online: 20 September 2025

*** Corresponding Author Email, crajeev238@gmail.com**

1, 2- School of Computer Science and Engineering, VIT-AP University, G-30, Inavolu, Beside AP Secretariat Amaravati, Andhra Pradesh-522237, India

Abstract
Anomalous Left Coronary Artery from the Pulmonary Artery (ALCAPA) is a series of congenital heart defects requiring precise image segmentation for accurate diagnosis. Existing research faced limitations such as loss of image detail, poor contrast handling, and vulnerability to noise leading to decreased accuracy. To address these challenges, this research introduces the High-Pitched Residual U-Network designed for automatic segmentation of ALCAPA from 3D Computed Tomography Angiography images. The proposed model integrates U-Net with residual blocks to extract low and mid-level features, mitigating information degradation. The encoder compresses the image using convolution, max-pooling, and dropout layers, while the decoder reconstructs the segmented image with Conv2DTranspose layers and residual block concatenation. Segmentation is performed using swish activation and sigmoid activation, with segmentation masks refined using Conditional Random Fields. The proposed method achieved an accuracy of 98.65% demonstrating a significant improvement over traditional method. This study highlights the potential of HPRUNET in transforming clinical diagnosis and treatment planning by automating the segmentation process, reducing manual intervention, and improving the detection of ALCAPA.

Keywords - ALCAPA, Medical Image segmentation, 3D Computed Tomography Angiography, Congenital heart disease, Deep Learning, High Pitched Residual U-Network (HPRUNET), Computed Tomography Angiography (CTA), Conditional Random Fields (CRFs)

INTRODUCTION

CAD is one of the world's most serious health issues, accounting for a sizable amount of morbidity and mortality. Despite significant advances in medical research and treatment choices, cardiovascular disease, especially coronary artery abnormalities, remains the leading cause of mortality worldwide [1]. These diseases impair the heart's capacity to deliver blood to essential organs, potentially leading to serious problems such as heart attacks, arrhythmias, and even sudden cardiac death. Among congenital cardiac anomalies, ALCAPA is particularly rare and dangerous, necessitating special treatment due to its distinct pathophysiology and potentially fatal effects if left untreated [2].

ALCAPA is a very rare congenital disorder, with an estimated frequency of 0.25–0.5% among congenital heart abnormalities. In this disorder, the left coronary artery (LCA), which is ordinarily responsible for providing oxygen-rich blood to the left side of the heart, emerges irregularly from the pulmonary artery (PA) rather than the aorta [3]. The PA generally transports oxygen-poor blood to the lungs for oxygenation, therefore in ALCAPA patients, the LCA receives and distributes deoxygenated blood to the heart muscle (myocardium). This causes significant oxygen deprivation, particularly in the left ventricle, which is crucial for pumping blood throughout the body [4]. As a result, the heart muscle may become ischaemic and begin to degenerate, leading to heart failure in newborns if not addressed promptly.

The clinical signs of ALCAPA vary depending on the severity of the illness and the formation of collateral blood arteries [5], which may compensate for the lack of oxygenated blood. Symptoms usually appear in infancy after the first few weeks of birth, as pulmonary pressures drop, limiting blood flow through the left coronary artery [6]. Infants may show indicators of heart failure, including difficulties eating, fast breathing, irritability, and poor weight gain. If left undetected, ALCAPA can cause serious problems such as myocardial infarction, congestive heart failure, mitral valve insufficiency, and arrhythmias [7-9]. The death rate for untreated ALCAPA is extremely high, with nearly 90% of newborns dying within the first year of life.

Early identification and surgical intervention are critical to improving outcomes for ALCAPA patients [10]. The goal of surgery is to restore normal coronary artery anatomy by re-implanting the left coronary artery into the aorta, which provides oxygenated blood to the heart muscle. When the problem is diagnosed early, the post-surgical outcomes are generally positive, with many patients going on to enjoy healthy lives after surgery [11-12]. However, delayed diagnosis frequently leads to irreparable cardiac injury, negatively impacting long-term prognosis and quality of life [13-14]. This emphasizes the importance of sophisticated imaging techniques and early detection of ALCAPA to limit the dangers associated with delayed therapy [15].

Echocardiography, CTA, and MRI are the primary imaging modalities used to accurately diagnose ALCAPA. Among these, CTA provides high-resolution pictures that enable thorough visualization of coronary architecture. Despite the efficiency of CTA, manual segmentation of coronary arteries, particularly in complex instances such as ALCAPA, is time-consuming and needs significant knowledge [16]. Manual segmentation increases the possibility of human error and can prolong the diagnosis and treatment process. As a result, automated segmentation algorithms capable of detecting coronary irregularities in CTA images have emerged as a major study topic.

To address the challenges of manual segmentation, this research introduces the novel DL model designed to automate segmentation of coronary arteries in ALCAPA patients. Thus, the proposed solution has the potential to improve the speed and accuracy of ALCAPA detection, ultimately leading to better patient outcomes and more efficient clinical workflows.

The main contributions of this research are as follows:

By addressing the unique challenges posed by this rare congenital heart condition, this research introduces a novel DL architecture as HPRUNET to segment the coronary arteries in patients with ALCAPA using 3D CTA images.

HPRUNET integrates U-Net and ResNet neural network architectures for image segmentation, improving accuracy and reducing overfitting in small datasets, particularly in complex structures like coronary arteries.

The research employs a sophisticated preprocessing pipeline to enhance the quality of input images and the model's performance, including data magnification, contrast enhancement, and noise reduction, to handle dataset variability and produce more reliable segmentation results.

The research uses L2 regularization and weighted Dice loss to address the challenges of small datasets and class imbalance in ALCAPA, ensuring stable and accurate segmentation results, even on underrepresented classes within the dataset.

The rest of the manuscript is structured as follows: the second section reviews existing segmentation methods using DL highlighting their limitations and the need for improved techniques. The third section describes the architecture of proposed methodology. The outcomes of the suggested method's implementation are covered in the fourth section. The major conclusions are summarized in section five.

LITERATURE SURVEY

Kong et al. [17] developed a new tree-structured convolutional gated recurrent unit (ConvGRU) model for learning the coronary artery's anatomical structure. This model accounts for local spatial correlations in input data, making it suitable for image analysis. The framework includes a fully convolutional network for feature extraction and predictions and a ConvGRU layer for modeling anatomical structures. However, the model faces limitations such as complexity and potential computational inefficiency when applied to larger datasets or real-time settings.

Yang X et al. [18] developed a geometry-based cascaded segmentation method for the coronary artery, addressing the challenge of complex structures and low resolution in medical images. They designed a cascaded network that integrates geometric deformation networks, producing precise meshes without fragmentation. They also reconstructed a finer, vectorized mesh with regularized morphology, improving the performance of the geometry-based segmentation network. They collected a dataset called CCA-200, which was annotated by radiologists, and verified the method on both the CCA-200 dataset and the public ASOCA dataset. However, its reliance on complex geometric transformations, may limit its adaptability to other anatomical structures.

Yang Y et al.[19] conducted a study to predict myocardial ischemia in patients with coronary heart disease using radiologic features from coronary computed tomography angiography (CCTA) combined with clinical factors. The study analyzed 110 patients who underwent CCTA scans before digital subtraction angiography (DSA) or fractional flow reserve (FFR) examinations. The patients were divided into two groups: myocardial ischemia and normal myocardial blood supply. The study faced limitations, including a small sample size, selection bias, and insufficient reliance on CCTA and clinical data, suggesting the need for additional data.

A study by Secinaro et al. [20] showed that cardiovascular magnetic resonance (CMR) is a valuable tool for assessing young patients after surgical repair of ALCAPA. The study involved six patients aged 9-21 years who underwent CMR due to clinical suspicion of myocardial ischemia. The findings revealed basal and anterolateral sub-endocardial myocardial fibrosis as a characteristic finding. However, the study's small sample size may limit its generalizability.

Castaldi et al. [21] conducted a study to detect regional left ventricular dysfunction, potentially predicting coronary lesions or residual myocardial fibrosis using speckle tracking. The study involved ten patients who underwent surgical re-implantation of the left coronary artery for ALCAPA. The researchers used S-SR imaging, cardiac MRI, and coronary angiography to evaluate functions and assess myocardial fibrosis and coronary anatomy. The study had limitations, including a small number of patients due to rare pathology and difficulty enrolling a large number at a single center.

Krokovay et al. [22] explored surgical reconstructive methods for non-sclerotic proximal coronary artery stenosis, including post-coronary artery transfer and de novo approaches. They developed a technique for anatomically reconstructing ostial and short-segment stenosis and atresia in infants using patch plasty or interposition vein grafts, aiming to restore natural coronary blood flow and facilitate future bypass operations. However, it may not be broadly generalizable to all coronary artery conditions.

A study by Jinmei et al. [23] found that most diagnoses of acute coronary syndrome (ALSAPA) in children occurred during childhood or adolescence, with advancements in imaging technology potentially enabling earlier detection. The study recommended increased suspicion of ALCAPA when echocardiograms showed retrograde flow or an enlarged right coronary artery. Early surgical intervention was emphasized for asymptomatic children or adolescents with ALCAPA. However, the study's retrospective diagnosis may have missed early cases and affected the accuracy of conclusions.

Zeng et al. [24] created the first 3D CTA image dataset for ALCAPA, using a multi-task 2D–3D ensemble technique. Their approach outperformed existing coronary artery segmentation techniques, but there's room for improvement. However, the small size of the dataset may limit its generalizability and robustness.

This review collectively advances the understanding and methods for ALCAPA segmentation and diagnosis. While innovative techniques and datasets have shown promise limitation such as small sample sizes and dataset constraints highlight the need for further research to enhance generalizability and accuracy in clinical applications.

PROPOSED METHODOLOGY

ALCAPA is a congenital cardiac anomaly where the left coronary artery originates from the pulmonary artery, leading to inadequate blood supply to the heart muscle, potentially causing early-onset heart failure and death if untreated. Early detection and accurate segmentation in medical imaging are crucial for timely intervention and management. The main aim of this research work to improve the accuracy and efficiency of ALCAPA detection and segmentation in medical images by addressing existing limitations and proposing a novel approach that integrates advanced pre-processing and segmentation strategies. The goal is to develop a robust model that aids clinicians in making precise diagnoses and treatment decisions. Existing research on ALCAPA detection and segmentation faces several challenges. Many methods lack crucial pre-processing steps, resulting in irrelevant and noisy features, increasing computational complexity, and reducing learning accuracy. Traditional architectures, with numerous parameters and skip connections, can over fit, affecting generalization. Standard loss functions are sensitive to class imbalance, leading to biased optimization and poor performance for minority classes. To address these

limitations, this research introduces HPRUNET a novel approach that integrates enhanced pre-processing techniques with a refined segmentation architecture which is shown in Figure 1.

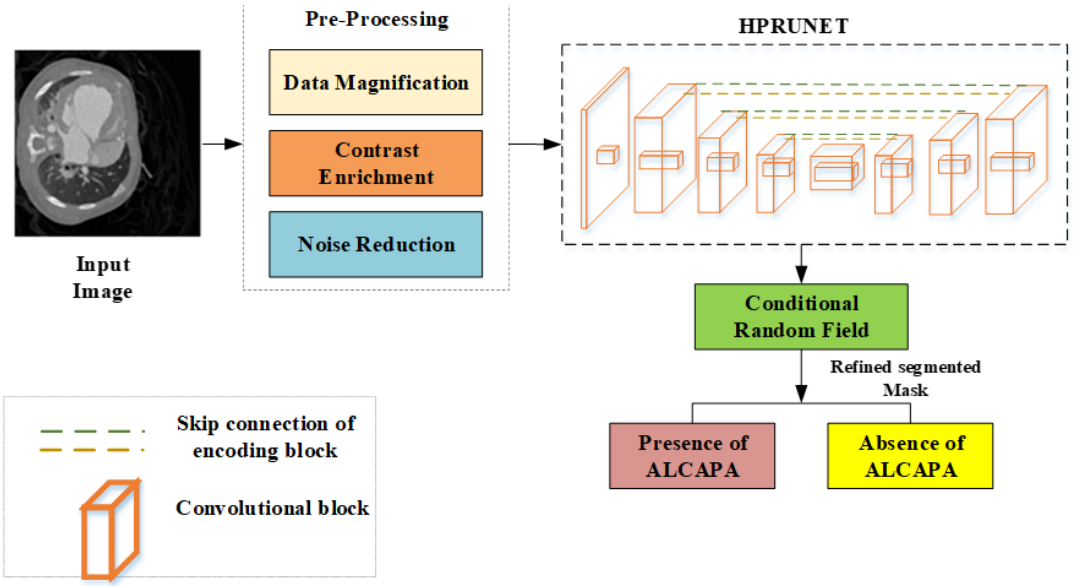

FIGURE 1
BLOCK DIAGRAM REPRESENTATION OF PROPOSED METHODOLOGY

This proposed methodology improves the accuracy and reliability of ALCAPA detection in medical imaging by combining advanced pre-processing with a sophisticated segmentation approach. The model uses random transformations to generalize better and adapt to varied image contexts. Contrast Limited Adaptive Histogram Equalization (CLAHE) is used instead of traditional histogram equalization to preserve image detail and maintain dynamic range. Bilateral Filtering is employed to smooth images while preserving edges, reducing noise, and enhancing image quality. Following this, the architecture integrates U-Net encoding and residual blocks to extract and refine features, mitigating information degradation and controlling overfitting. The decoder block performs feature expansion, while Conditional Random Fields (CRFs) are used to refine the segmentation mask. Weighted Dice loss is used to address class imbalance by assigning higher weights to underrepresented classes. The methodology offers several advantages over existing approaches, including enhanced accuracy, reduced overfitting, and better handling of class imbalance.

I. Pre-processing

This work emphasizes the importance of robust pre-processing techniques to improve the accuracy of ALCAPA detection in medical images. To address the challenges of noisy and low-contrast images, this proposed approach incorporates Data Magnification, Contrast enrichment, and noise reduction techniques ensuring more precise segmentation and better overall model performance.

I.I. Data Magnification

It can involve applying random transformations such as rotating, flipping, cropping, and scaling ratio to expand the training data represented in Algorithm 1, thereby aiding proposed models in learning patterns effectively and becoming more robust in image segmentation which includes rotation, flipping, cropping and diversity of input images to enhance the quality and diversity of input images, thus improving model generalization and segmentation accuracy. The combination of these techniques effectively addresses the limitations of noise, contrast and variation in ALCAPA images, making it practical improvement over existing pre-processing methods.

- *Rotation*

Rotation of an input image involves changing the orientation of the image by a certain angle (θ). It is represented by a matrix; rotation can be achieved using rotation matrices. The rotation matrix for an image transformation is;

$$\begin{bmatrix} \cos(\theta) & -\sin(\theta) \\ \sin(\theta) & \cos(\theta) \end{bmatrix} \quad (1)$$

Where, θ represents the angle of rotation in radians, and $\mathbf{cos}(\theta)$ and $\mathbf{sin}(\theta)$are the cosine and sine of the angle, respectively. Given a point in the original image with coordinates (x, y), the coordinates of the point after rotation (x', y') by angle θ would be:

$$\begin{bmatrix} x' \\ y' \end{bmatrix} = \begin{bmatrix} \cos(\theta) & -\sin(\theta) \\ \sin(\theta) & \cos(\theta) \end{bmatrix} \begin{bmatrix} x \\ y \end{bmatrix} \quad (2)$$

- *Flipping*

It is an image horizontally or vertically that involves changing the arrangement of pixels. For a horizontal flip, the transformation is represented as;

$$x' = W - 1 - x;\ y' = y \quad (3)$$

Where $x\ and\ y$the original coordinates of a pixel, W is H represents the picture's size, and W is its width. For a vertical flip, the transformation is:

$$x' = x;\ \ y' = H - 1 - y \quad (4)$$

Flipping the image helps the model to understand objects irrespective of their orientation.

- *Cropping*

It involves removing parts of the image outside a specified region. If an image has dimensions $W \times H$ and the cropped region has coordinates $(x_1 \times y_1)$ as the top-left corner and $(x_2 \times y_2)$ as the bottom-right corner, the cropped image would have dimensions $(x_2 - x_1) \times (y_2 - y_1)$. This aids the model in concentrating on particular regions of attention within the picture. Improving its ability to recognize relevant features.

- *Scaling ratio*

Scaling an image involves changing its size while maintaining its aspect ratio. The scaling factor s for both width and height can be applied to resize the image.

$$New\ width = Original\ width \times s;\ New\ height = Original\ height \times s \quad (5)$$

This transformation allows the model to learn from objects at different scales, enhancing its robustness. These image transformations play crucial roles in magnification datasets for training proposed models and enhancing their ability to generalize across various scenarios and orientations.

Algorithm 1: Data Magnification

Step 1: Apply random transformation (input image)
if choice == 0:
    Rotate the image by a certain angle (θ)
    Angle = random uniform
    Height and width = image shape
    Rotation matrix using equation (1)
else if choice ==1:

Step 2: Flip the image horizontally or vertically
Horizontal flip transformation using equation (3)
Vertical flip transformation using equation (3)
else if choice ==2:
Step 3: Crop a random portion of the image
Height, width = image shape
Coordinates (x_1 ×y_1), (x_2 ×y_2) as the top-left and bottom-right corner
Cropped image dimension as (x_2 -x_1)×(y_2 -y_1)
else if choice ==3:
Step 4: Scale the image by random ratio
Scale ratio using equation (5)
Output: Augmented image

Hence, the data magnification assists the proposed model in generalizing better and improving its ability to detect and segment the images in different contexts. Then, to enrich the contrast in the augmented image the existing research utilized histogram equalization, however, it stretches the pixel values to cover the entire range of possible values, which may reduce the dynamic range, which may lead to Loss of information and detail.

I.II. Contrast Enrichment

It is an advanced technique designed to improve the local contrast of an image. Unlike traditional histogram equalization which stretches the pixel values uniformly across the entire image, CLAHE operates on small regions called tiles within the image. This prevents the over-amplification of noise and avoids over-stretching of pixel values which can result in loss of detail in bright or dark areas. Additionally, CLAHE preserves finer details and maintains a more balanced dynamic range leading to clearer and more informative images whose process steps are analyzed in Algorithm 2.

Five primary processes comprise the CLAHE pipeline: bilinear interpolation, histogram correction, mapping function, and picture breakdown into rectangular pieces. The image is divided into blocks, and then a histogram is made, clipped, and redistributed. The histogram's peak value is clipped off at the clip point, and the clipped pixels are then dispersed throughout the various grey levels. More contrast is added the higher the clip point.

$$\beta = \frac{M}{N}\left(1 + \frac{\alpha}{100} S_{max}\right) \tag{6}$$

The clip factor, or α, is a crucial element for adjusting contrast enhancement in image blocks. When α gets closer to 100, the contrast increases significantly, yet the clip point remains constant when α gets closer to 0. A mapping function based on CDF is produced, which adjusts the dynamic range and pixel size to remap the grey levels of image blocks.

$$cdf(l) = \sum_{k=0}^{l} pdf(l) \tag{7}$$
$$T(l) = cdf(l) \times l_{max} \tag{8}$$

Where T (l) is the remapping function, l max is the maximum pixel value in the block, and l is the pixel grey level. In each block, the CDF of the redistributed histogram yields a variety of remapping functions. To get over blocking limitations, each pixel value is interpolated from the mapping functions in the nearby blocks.

Algorithm 2: Contrast Limited Adaptive Histogram Equalization

Input: Augmented Image
Step 1: Tile processing
- *For each tile:*
- Compute the histogram of pixel intensities
- Clip the histogram if any bin exceeds the clip limit.
- Perform histogram equalization on the clipped histogram.

Map the pixel values according to the equalized histogram.
Step 2: Boundary Interpolation
Smooth the transitions between adjacent tiles using bilinear interpolation.
Step 3: Reconstruct image
Combine all processed tiles to form the enhanced image.
Step 4: Adjust Dynamic Range
Ensure that the final image maintains a balanced dynamic range and proper brightness.

Therefore, CLAHE shown in Figure 2 compares the original image with the contrast-enhanced version achieved using CLAHE. It shows how CLAHE improves local contrast making details that were previously hard to distinguish more visible. Thus the enhanced image maintains a better dynamic range providing clearer and more defined features which is essential for accurate segmentation.

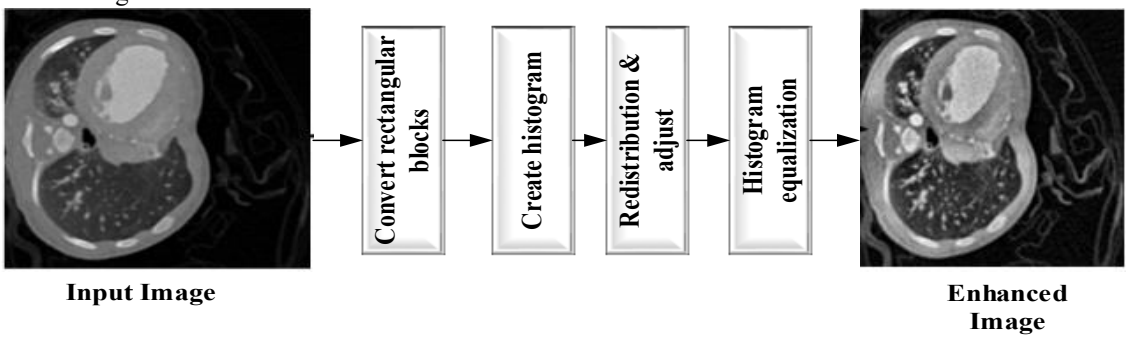

FIGURE 2
RESULTS OF THE ENHANCED IMAGE USING CLAHE APPROACHES

I.III. Noise Reduction

For enhancing contrast, CLAHE achieves minimal computational cost because of the independent processing of blocks. Moreover, the enhanced images have some noise, therefore, to reduce the noise, this research utilized bilateral filtering which is employed to smooth the image while preserving edges, reducing noise, and enhancing image quality. It preserves edges by considering both the spatial distance between pixels and the intensity difference of pixel values by using two Gaussian filters. One based on the spatial proximity of neighboring pixels and another based on intensity differences. This dual consideration ensures that nearby pixels with similar intensities contribute more to the filtered pixel.

The filter operates over a local window or neighborhood for each pixel (x_0, y_0) in the image, calculating the spatial weight W_s based on the Euclidean distance between the center pixel (x_0, y_0) and a neighboring pixel. This weight is determined by the Gaussian function, ensuring accurate and consistent image quality.

$$W_s(x_0, y_0, x, y) = exp\left(-\frac{(x_0-x)^2+(y_0-y)^2}{2\sigma_s^2}\right) \quad (9)$$

Where σ_s controls how much weight is given based on the distance between pixels. Closer pixels will have higher spatial weights.

Next, the intensity weight W_r is calculated based on intensity difference between the center pixel $I(x_0, y_0)$ and the neighboring pixel $I(x, y)$ is given by,

$$W_r\big(I(x_0,y_0),I(x,y)\big) = exp\left(-\frac{(I(x_0,y_0)-I(x,y))^2}{2\sigma_r^2}\right) \quad (10)$$

Where σ_r controls how sensitive the filter is to intensity differences. Pixels with similar intensities are given higher weights, while those with larger intensity differences contribute less to the final result.

The bilateral combines these two weights to compute the output intensity for the pixel $I'(x_0,y_0)$ using the weighted sum,

$$I'(x_0,y_0) = \frac{\sum_{(x,y)\in Neighborhood} W_s(x_0,y_0,x,y).W_r\big(I(x_0,y_0),I(x,y)\big).I(x,y)}{\sum_{(x,y)\in Neighborhood} W_s(x_0,y_0,x,y).W_r\big(I(x_0,y_0),I(x,y)\big)} \quad (11)$$

Equation (11) ensures that the intensity of output pixel $I'(x_0,y_0)$ is a weighted average of the intensities in its neighborhood with more influence from pixels that are both spatially close and similar in intensity. This step ensures that the image is clean and well-defined facilitating better segmentation in subsequent processing steps. Figure 3 demonstrates the effect of bilateral filtering on the input image.

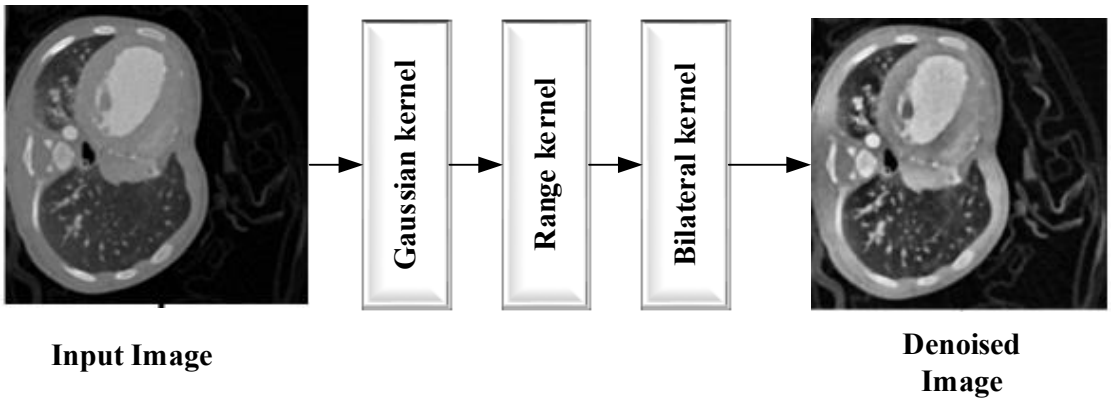

FIGURE 2
NOISE REDUCTION PROCESS RESULTS USING BILATERAL FILTERING

II. Proposed Model HPRUNET

Following that pre-processing, to segment the ALCAPA this research proposed a novel HPRUNET: High Pitched Residual U-Network which is tailored for automatic segmentation of coronary arteries in patients with ALCAPA using 3D CTA images. It is designed to enhance segmentation accuracy and mitigate the limitations encountered in previous methods such as overfitting and degradation. In the proposed architecture, these two networks are integrated. The 256x256 input images are produced via the proposed HPRUNET design, which is shown in Figure 4, using broad and residual context blocks.

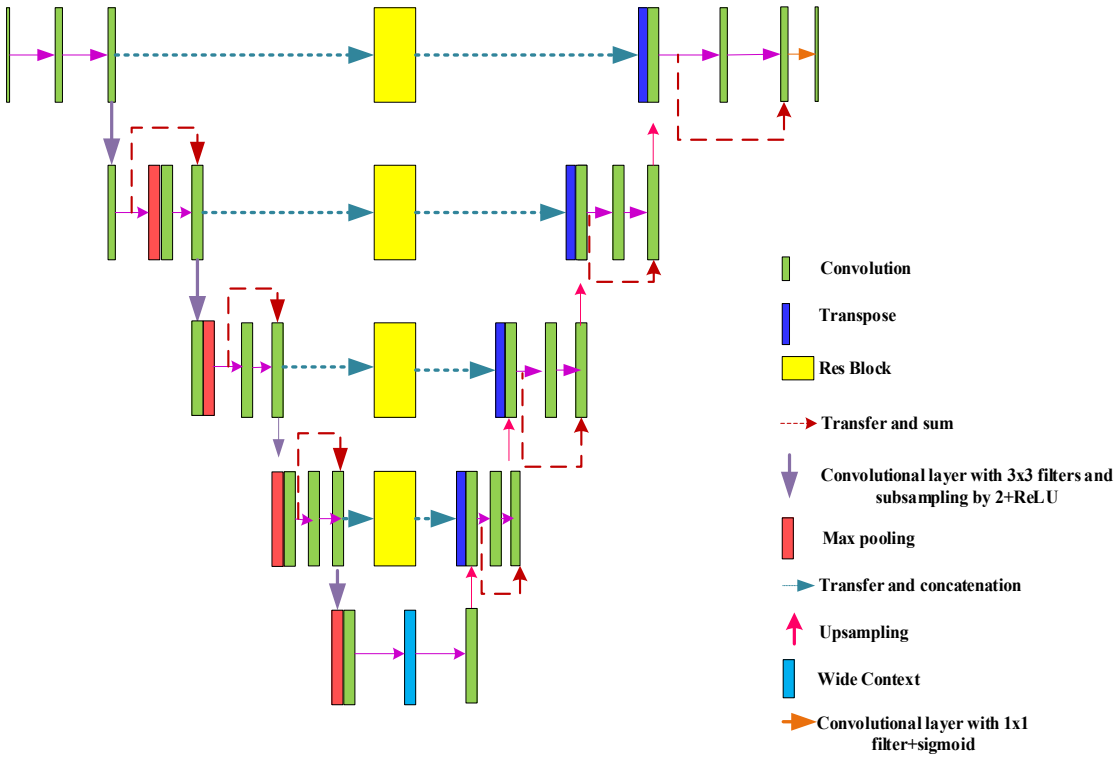

FIGURE 3
ARCHITECTURE OF HPRUNET

The core structure of HPRUNET integrates UNet's robust segmentation architecture with residual connections to overcome the problem of vanishing gradients, a common issue in deep networks, especially when dealing with complex medical images. U-Net is known for its encoder-decoder design, in which the encoder harvests features via down sampling and the decoder reconstructs the segmentation map via up sampling. Skip connections in U-Net are effective at retaining spatial information between layers, which is essential for correct segmentation. However, U-Net alone may suffer from information degradation due to network depth, resulting in inadequate feature extraction, particularly when dealing with fine details in medical pictures such as coronary arteries. To counteract this, leftover blocks are incorporated into the architecture. Residual connections enable the network to transmit data straight from one layer to another, skipping intermediary layers. This helps to avoid the vanishing gradient problem and enables the network to learn deeper, more abstract properties while retaining low-level details. The architecture of the Residual Extended Skip (RES) block is shown in Figure 5. The residual blocks also enable more efficient gradient flow during backpropagation, hence increasing the network's convergence speed and stability. The architecture employs standard convolutional layers in both the encoder and decoder sections, with each residual block consisting of two convolutional layers and skip connections. These blocks guarantee that the network maintains a rich flow of information between layers, preserving critical details required for accurate segmentation of small and complex locations like coronary arteries.

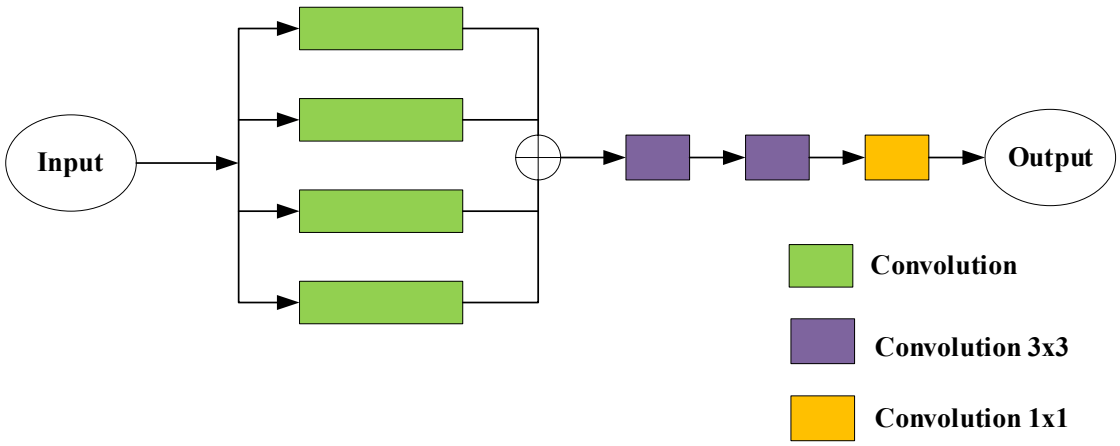

FIGURE 4
ARCHITECTURE OF RES BLOCK

HPRUNET has introduced a Wide Context Block (WCB) to improve its ability to capture global contextual information, particularly crucial for segmenting intricate structures like coronary arteries. Traditional U-Net convolutional layers process only a small portion of input, limiting their ability to capture the broader context needed for accurate segmentation in complex medical images. The WCB overcomes this limitation by expanding the receptive field and incorporating multi-scale features. It achieves this by employing dilated convolutions, enabling the network to extract features at many scales while minimizing the parameters. Dilated convolutions create gaps between sampled points in the receptive field, allowing the network to evaluate a broader portion of the image while retaining feature resolution. The dilation rate is regulated at each layer to gradually enlarge the receptive field, catching both local features and broader contextual information needed to discern between locally situated structures like coronary arteries and surrounding tissues.

Mathematically, the dilated convolution operation for a filter k and dilation rate r is represented as,

$$y[i] = \sum_{j=0}^{k-1} x[i + r.j]w[j] \tag{12}$$

Where x is the input feature map, w is the filter and $y[i]$ is the output feature map. The dilation rate r controls the spacing between the filter weights, allowing the network to aggregate information over a wide area without down sampling the image. Thus, WCB improves HPRUNET by offering a more complete comprehension of the image, making it especially useful for segmenting small structures such as coronary arteries, which necessitate both detailed local feature extraction and larger contextual awareness. The WCB reduces false positives and negatives in segmentation tasks by capturing global information, which is especially useful in difficult circumstances where the limits of the arteries are not clearly distinguished from surrounding tissue.

The scarcity of large, labelled datasets poses a significant challenge in medical imaging, particularly for rare conditions such as ALCAPA. Small datasets pose a high risk of overfitting, which occurs when the model gets overly specialized on the training data and needs to generalize to new data. HPRUNET incorporates several strategies to mitigate the risk. First, L2 regularisation is applied to the network's weights, penalizing large weights and encouraging the model to focus on more generalized patterns in the data, reducing overfitting. This regularisation technique includes a loss term that is proportional to the total of the squared weights.

$$L_{reg} = \lambda \sum_i w_i^2 \tag{13}$$

Where λ is the regularization strength and w_i represents the weights of network. This term is added to the primary loss function to discourage excessively large weight values, promoting better generalization.

In addition to regularisation, HPRUNET handles class imbalance, a prevalent problem in medical Image segmentation in which regions of interest (for example, coronary arteries) may occupy just a small fraction of the image compared to the backdrop. Standard loss functions, such as cross-entropy, can cause biased optimization in favor of the majority class

(background pixels), resulting in poor performance in the minority class (artery pixels). To solve this, the network uses a weighted Dice loss function:

$$L_{Dice} = 1 - \frac{2\sum_i w_i p_i g_i}{\sum_i w_i (p_i + g_i)} \tag{14}$$

Where P_i represents the predicted segmentation probabilities, g_i represents the ground truth and w_i are the weights assigned to each class giving more importance to underrepresented classes. The weighted Dice loss ensures that the model prioritizes the accurate segmentation of minority regions, such as coronary arteries, improving performance on small structures.

Thus, the integration of U-Net and residual blocks within HPRUNET allows the model to effectively balance low-level and high-level feature extraction. By preserving both fine details and more abstract features, the model enhances segmentation accuracy while handling limited data and demonstrates its robustness and reliability making it an effective tool for clinical applications. The results clearly show the predicted results for ALCAPA detection from HPRUNET model represented in Figure 6.

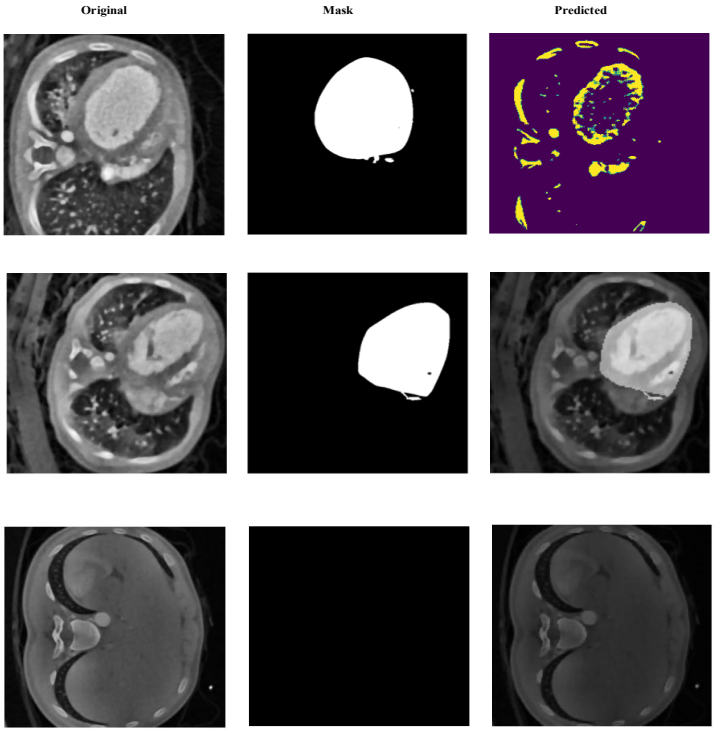

FIGURE 5
ALCAPA PREDICTED RESULTS USING THE PROPOSED MODEL

From the above-segmented results, the presence of ALCAPA is demonstrated by exhibiting the original input image, its related ground truth mask, and the model's anticipated segmentation output. This demonstrates the model's capacity to effectively recognize and segment aberrant coronary arteries in complex medical imagery. The mask image depicts an instance in which ALCAPA is absent. Similar to the preceding panel, it includes the original input image, the ground truth mask indicating no abnormality, and the model's predicted image. The absence of ALCAPA is properly diagnosed, demonstrating the model's ability to distinguish between normal and aberrant cases.

RESULTS AND DISCUSSION

The proposed HPRUNET model was evaluated on an ALCAPA dataset for the task of identifying aberrant coronary arteries in 3D CTA images. The model was developed in Python 3 on a Windows 10 (64-bit) operating system with an Intel Pentium

processor and 16GB RAM. Despite the limited hardware, the model was optimized for performance using efficient hyperparameter tuning. The list of hyperparameters used in this research is represented in Table I.

TABLE I
HYPERPARAMETERS OF PROPOSED APPROACH

Parameter	**Value**
Image dimensions	256×256
Batch size	32
Learning rate	0.0001
Loss	Binary cross entropy
Activation	Swish
Encoding	
Convolution	64, 128, 256, 512, 1024
Kernel size	3×3
Padding	Same
Kernel regularizer (L2)	0.01
Pooling	Max-pooling
Pooling size	2 × 2
Dropout	0.25
Normalization	Batch normalization
Decoding	
Convolution	512, 256, 128, 64
Kernel size	2×2
Strides	2×2
Padding	Same

The results demonstrated that HPRUNET accurately segmented the ALCAPA regions in the images. Swish activation throughout the network improved the model's performance by producing smooth gradients and enhancing convergence. Previous models struggled with overfitting, but the combination of Binary Cross-Entropy loss and L2 regularisation prevented it, especially on the small dataset. Batch normalization after each convolutional layer increased the model's stability and performance throughout the training phase. During the encoding phase, the model's increasing number of filters (64 to 1024) allowed it to capture complicated characteristics, while the Max-pooling layers reduced dimensionality and highlighted the most important sections of the image. During the decoding phase, transposed convolutions with gradually decreasing filter sizes (512 to 64) allowed the network to recreate tiny details in the image which is required for precision segmentation.

The results showed that the HPRUNET model successfully mitigated the challenges of overfitting and data degradation by utilizing residual connections and Wide Context Blocks. Furthermore, weighted Dice loss enhanced the handling of class imbalance, resulting in superior segmentation performance for smaller and less-represented sections of the coronary arteries.

I.Dataset Description

The ALCAPA dataset contains medical imaging data used to study and detect ALCAPA, a rare congenital cardiac abnormality. The dataset contains a series of 3D Coronary CT Angiography (CTA) scans, which are essential for detecting the abnormal connection between the left coronary artery and the pulmonary artery. These images capture the fine intricacies of coronary artery architecture, making them essential for precise segmentation tasks. This dataset consists of thirty 3D CT images collected at Guangdong Provincial People's Hospital using a SOMATOM Definition Flash CT scanner. These images are obtained between June 2016 and August 2021, providing a comprehensive view of the condition. The dataset focuses on axial pre-operative CTA images of neck and brachiocephalic arteries which are essential for diagnosing ALCAPA. Segmentation labeling for this dataset was carried out by two experienced cardiovascular radiologists with specialized knowledge of ALCAPA. Their collaboration ensures the precision and accuracy of segmentation making the dataset a valuable resource for training 80% and testing 20% automatic segmentation models for this congenital anomaly. The additional image consists of the original image paired with a mask image generated using the L2 regularizer method as shown in Figure 7.

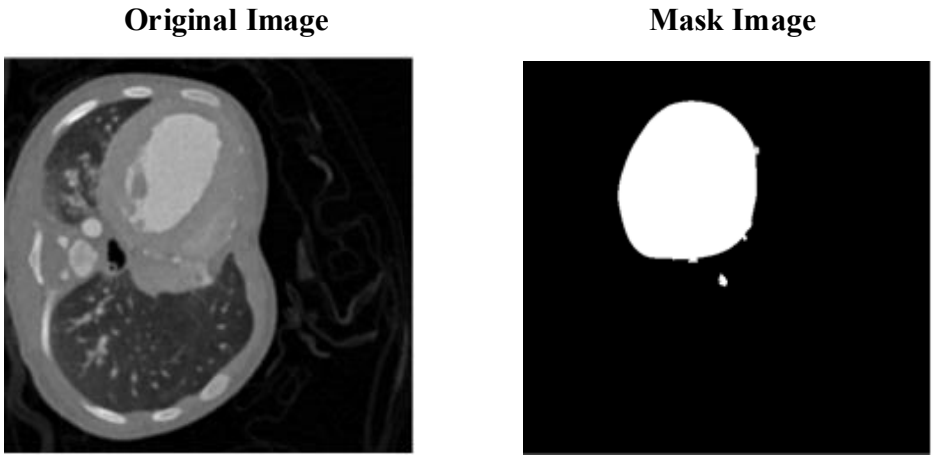

FIGURE 6
SAMPLE IMAGE FROM DATASET

II. Performance Metrics

In the evaluation of medical image segmentation models, various metrics are employed to assess the effectiveness of the proposed method, particularly for detecting and segmenting ALCAPA from 3D CTA images. The model performance was validated through a series of following quantitative metrics. The results were tracked across multiple epochs and the performance was compared against existing approaches. Cross validation techniques were also employed to ensure the model generalized well to unseen data reducing the likelihood of overfitting. Additionally, visual inspection of predicted segmentation results further validated the model's accuracy in detecting and segmenting ALCAPA.

1. Accuracy

It measures the overall correctness of model by calculating the ratio of correctly predicted instances (true positives and negatives) to the total number of predictions. FOR ALCAPA detection, it indicates how well the model can correctly identify both the presence and absence of ALCAPA across the dataset.

$$Accuracy = \frac{TP+TN}{TP+TN+FP+FN} \tag{15}$$

2. Sensitivity (sens)

It is also known as recall or true positive rate measures the model's ability to correctly identify positive instances (the presence of ALCAPA). A higher sensitivity value indicates that the model effectively detects ALCAPA cases, minimizing the FN.

$$Sens = \frac{TP}{TP+FN} \tag{16}$$

3. Hausdorf Distance (HD)

It evaluates the extent to which the model's segmentation results deviate from the ground truth. It quantifies the maximum distance between the predicted segmentation's boundary points and the segmentation mask. A lower HD shows better alignment between predicted and true segmentations, showing the model's accuracy in boundary recognition.

$$Hausdorff\ distance(A,B) = max(max(dist(a,B)), max(dist(b,A))) \tag{17}$$

Dist. (a, B) represents the separation between points 'a usual A and any point in set B, and 'b' in fixed B and any point in set A.

4. Dice Similarity Coefficient (DSC)

It is a prominent metric for determining the overlap between the predicted segmentation and the ground truth. It is especially beneficial for medical image segmentation, which requires exact overlap. The Dice score ranges from 0 to 1 where 1 represents perfect overlap.

$$DSC = \frac{2 \times TP}{2 \times TP + FP + FN} \tag{18}$$

Thus, the performance of proposed HPRUNET model was evaluated over multiple epochs with results presented in terms of training loss, accuracy, sensitivity, DSC, HD for both training and validations set. Table II provides a detailed summary of model progression through first three epochs.

TABLE II
PERFORMANCE METRICS RESULTS FOR TRAINING AND VALIDATION OBTAINED FROM THE PROPOSED MODEL

Epochs	Training					Validation				
	Loss	Acc	Sens	DSC	HD	Loss	Acc	Sensitivity	DSC	HD
1	0.8196	0.5229	0.8484	0.1744	25.45	0.757	0.2508	0.9998	0.2289	29.992
2	0.7010	0.7841	0.8406	0.3064	25.21	0.755	0.3307	0.9997	0.2551	29.990
3	0.6355	0.9134	0.7324	0.7061	21.97	0.749	0.4383	0.9973	0.3009	29.918

The model's training accuracy and sensitivity were moderate in the first epoch, with a high sensitivity of 84.84%. However, the model's segmentation was not yet accurate, with significant differences between predicted and actual boundaries. The validation set showed a low

Accuracy of 25.08% but almost perfect sensitivity of 99.98%. The accuracy graph is represented in Figure 8, the model achieved 98.65%.

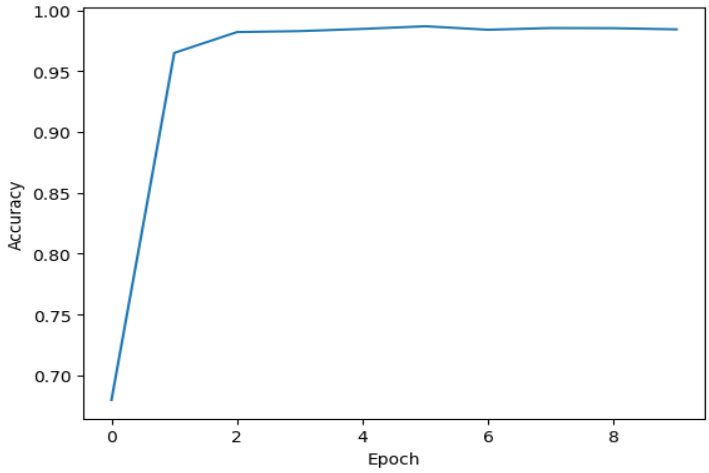

FIGURE 7
ACCURACY OF PROPOSED APPROACH

In the second epoch, the training accuracy improved significantly to 78.41%, with a slightly reduced DSC and HD. The model's accuracy increased to 33.07% on the validation set, but still showed high sens (99.97%), confirming its tendency to over-segment positive cases.

In the third epoch, the model reached a training accuracy of 91.34%, with a significantly increased DSC and a drop in HD. The model's accuracy increased to 43.83% on the validation set, and the Dice coefficient improved to 30.09%, with sensitivity still near-perfect at 99.73%.

The model's continuous improvement in both training and validation metrics was likely due to the use of Weighted Dice loss and Bilateral Filtering. This gradual improvement in accuracy and segmentation quality demonstrates the model's ability to learn more effectively with each epoch, addressing early concerns of overfitting and poor boundary detection.

III. Comparative Analysis

This research compares with existing methods from the study [24] including 2D U-Net and alternative approaches labelled as Method A, Approach B, and Approach C, as well as combinations of these methods with 2D U-Net which focusing on three metrics such as DSC, Sens, HD. The comparison results are shown in Table III.

TABLE III
PERFORMANCE COMPARISON OF DIFFERENT SEGMENTATION APPROACHES

Models	DSC (%)	Sens (%)	HD (mm)
2D U-Net	0.58±0.13	0.52±0.17	44.77±20.68
Method A	0.51±0.13	0.48±0.16	66.78±44.89
Approach B	0.47±0.15	0.48±0.17	87.43±60.29
Approach C	0.59±0.11	0.54±0.13	55.98±35.79
2D U-net Method A	0.60±0.12	0.63±0.17	56.67±36.79
2D U-net Method B	0.57±0.15	0.59±0.17	84.92±76.55
2D U-net Method C	0.65±0.11	0.65±0.16	53.64±34.34
Proposed	0.72±0.05	0.846±0.03	23.4±1.0

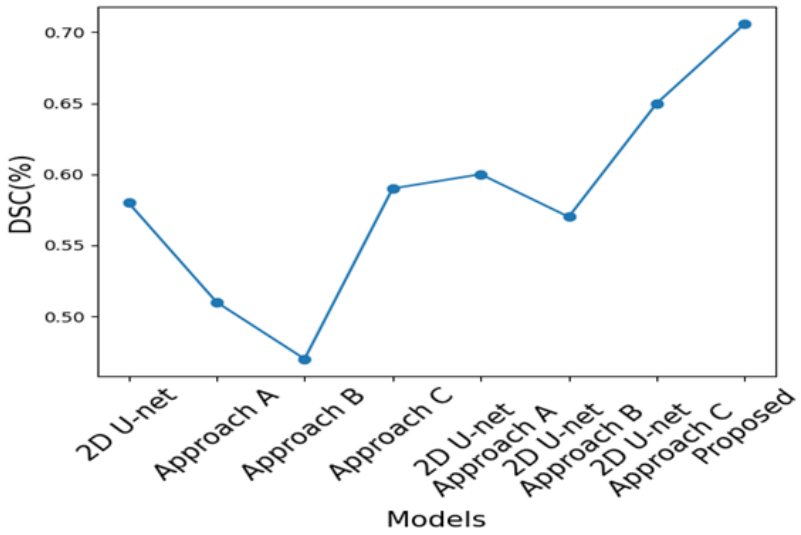

FIGURE 8
DSC COMPARISON

DSC evaluates the overlap of expected and ground-truth segmentations whose comparison graph is represented in Figure 9. The proposed technique had the highest DSC score (0.72±0.05), indicating exceptional segmentation performance. Compared to other techniques, 2D U-Net (0.58±0.13) and Approach B (0.47±0.15) showed lower DSC values, indicating less overlap between predicted and actual segmentation. The closest rival, 2D U-net Method C, had a DSC of 0.65±0.11, which is still lower than the proposed method. Additionally, Sensitivity assesses the capacity to appropriately identify affirmative cases (ALCAPA areas). The suggested model has the best sensitivity (0.846±0.03), indicating its capacity to detect ALCAPA with low false negatives. Method A (0.48±0.16) and Approach B (0.48±0.17) have significantly lesser sensitivity. The highest-performing rival, 2D U-net Method C, had a sensitivity of 0.65±0.16, which was much lower than the proposed model's results. The comparison of sensitivity is represented in Figure 10.

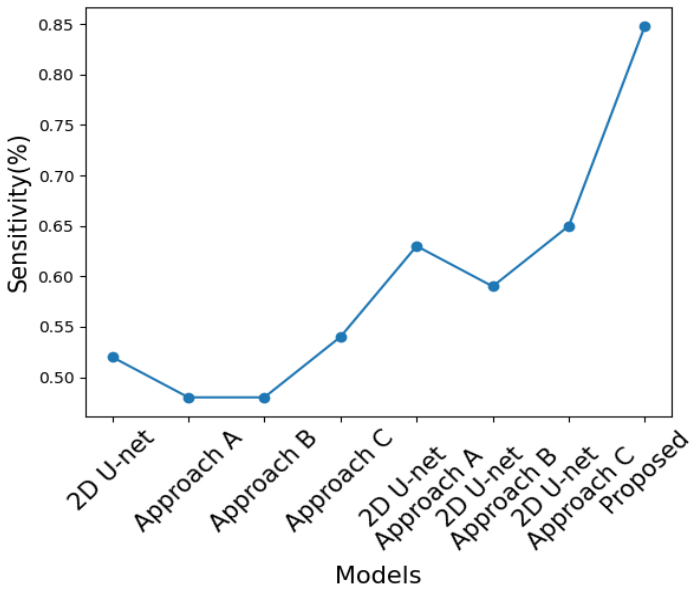

FIGURE 9
SENSITIVITY COMPARISON

Also, HD calculates the maximum gap between anticipated and ground-truth limits, with lower values indicating better alignment. The proposed model outperformed other techniques, with an HD of 23.4±1.0 mm. Approach B showed the worst HD (87.43±60.29 mm), indicating poor boundary identification. The suggested model outperformed 2D U-net Method C, a stronger competition, with a higher HD value of 53.64±34.34 mm, indicating its superiority in preserving correct boundaries. The comparison result of HD is visually represented in Figure 11.

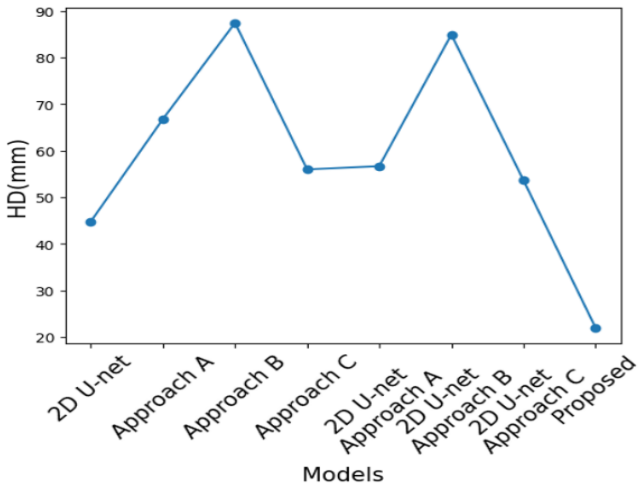

FIGURE 10
COMPARISON OF HD

This comparison shows that the proposed HPRUNET model outperforms standard approaches and their modifications in all three performance criteria. This increase indicates the model's capacity to precisely segment ALCAPA regions while also efficiently handling border precision, which is a hurdle for previous techniques. The combination of U-Net with residual blocks coupled with advanced techniques like weighted Dice loss and L2 regularization enables the proposed approach to excel in scenarios where previous approaches struggle especially in handling small datasets and complex anatomical structures.

This study describes a unique HPRUNET model for accurately segmenting ALCAPA in coronary artery pictures, which addresses major issues in medical image processing. The model enhances segmentation accuracy greatly by incorporating residual blocks into the U-Net architecture and using advanced pre-processing techniques like as contrast enhancement and bilateral filtering. The inclusion of weighted Dice loss and CRFs improves the model's performance, especially on small datasets with class imbalance. Experimental results show that the suggested strategy outperforms existing approaches in terms of accuracy and robustness. However, the model's performance may be influenced by the increased training time required due to its complex architecture.

CONCLUSION

In the realm of segmenting medical pictures, the HPRUNET represents a significant breakthrough, especially when it comes to the crucial duty of distinguishing the ALCAPA. It is noteworthy that it overcomes the enduring problem of overfitting and class imbalance, guaranteeing the maximum accuracy on a wide range of datasets. This research introduces the HPRUNET DL architecture to address these challenges by incorporating L2 regularization and weighted Dice loss. Its smooth integration with a residual network enhances its capabilities and offers an unmatched way to deal with problems related to class imbalance, resulting in performance that has never been seen before. Its consistent resilience and remarkable generalization over a variety of datasets were investigated in this research employing the Image ALCAPA dataset, which is a 3D CTA image data. Thus, the model achieves higher accuracy of 98.65% and sensitivity 84.6%. The results demonstrate significant improvements over traditional methods, making HPRUNET a promising approach for early and accurate ALCAPA detection. Future work will focus on expanding the dataset and exploring additional enhancements to further improve generalization and robustness.

REFERENCES

[1] Kumar, K. (2022). MDCT Evaluation of Congenital Coronary Anomalies: Pictorial Essay.

[2] Evangelista, M., Ferrero, P., D'Aiello, A. F., Negura, D., Micheletti, A., Bevilacqua, F., & Chessa, M. (2024). Coronary artery anomalies: what are they? when to suspect? how to treat? —a narrative review. Translational Pediatrics, 13(7), 1242.

[3] Aboshahba, A., Alttahan, A. H. A. M., Mokarrab, M., & Sadek, Y. (2021). Long term follows up after successful recanalization of coronary artery chronic total occlusion using antegrade versus retrograde approach by single photon emission computed tomography. Journal of Cardiology Research Review & Reports. SRC/JCRRR-138. DOI: https://doi. org/10.47363/JCRRR/2021 (2), 133, 3.

[4] Jiang, M., Xie, X., Cao, F., & Wang, Y. (2021). Mitochondrial metabolism in myocardial remodeling and mechanical unloading: implications for ischemic heart disease. Frontiers in Cardiovascular Medicine, 8, 789267.

[5] Kubota, H., Endo, H., Ishii, H., Tsuchiya, H., Inaba, Y., Terakawa, K., & Sudo, K. (2020). Adult ALCAPA: from histological picture to clinical features. Journal of Cardiothoracic Surgery, 15, 1-9.

[6] Menahem, S., Sehgal, A., & Wurzel, D. F. (2023). Persistent tachypnoea in early infancy: a clinical perspective. Children, 10(5), 789.

[7] López, D. E. S., Ynostroza, S. I. M., Rodríguez, K. V., Saldaña, M. K. L., Chávez, J. A. V., & Pimentel, X. A. A. (2024). Anomalous Left Coronary Artery from the Pulmonary Artery (ALCAPA) Syndrome: Pathophysiology, Clinical Manifestations, and Management Strategies. International Journal of Medical Science and Clinical Research Studies, 4(05), 953-959.

[8] Prandi, F. R., Zaidi, A. N., LaRocca, G., Hadley, M., Riasat, M., Anastasius, M. O., & Lerakis, S. (2022). Sudden cardiac arrest in an adult with anomalous origin of the left coronary artery from the pulmonary artery (ALCAPA): case report. International Journal of Environmental Research and Public Health, 19(3), 1554.

[9] Gondal, M. U. R., Nair, D. P. J. R., Shah, S., Zafar, M., Hanif, M. A., McCauley, B., & Hope, E. (2024). Myocardial Infarction and Complete Heart Block in a Patient with Anomalous Origin of the Left Coronary Artery from the Pulmonary Artery (ALCAPA). Cureus, 16(6).

[10] Cambronero-Cortinas, E., Moratalla-Haro, P., González-García, A. E., & Oliver-Ruiz, J. M. (2020). Case report of asymptomatic very late presentation of ALCAPA syndrome: review of the literature since pathophysiology until treatment. European Heart Journal-Case Reports, 4(5), 1-5.

[11] Pačarić, S., Turk, T., Erić, I., Orkić, Ž., Petek Erić, A., Milostić-Srb, A., ... & Nemčić, A. (2020). Assessment of the quality of life in patients before and after coronary artery bypass grafting (CABG): a prospective study. International journal of environmental research and public health, 17(4), 1417.

[12] Lourens, E. C., Baker, R. A., & Krieg, B. M. (2022). Quality of life following cardiac rehabilitation in cardiac surgery patients. Journal of Cardiothoracic Surgery, 17(1), 137.

[13] Samaras, A., Moysidis, D. V., Papazoglou, A. S., Rampidis, G., Kampaktsis, P. N., Kouskouras, K., & Giannakoulas, G. (2023). Diagnostic Puzzles and Cause-Targeted Treatment Strategies in Myocardial Infarction with Non-Obstructive Coronary Arteries: An Updated Review. Journal of Clinical Medicine, 12(19), 6198.

[14] Šulcová, J., & Murgová, A. (2020). Quality of life in patients after acute coronary syndrome in a lifestyle context. Україна. Здоров'я нації, 2(3).

[15] Xin, H., & Zhu, M. (2023). Imaging options for defining anomalous origin of the coronary artery from the pulmonary artery. Quantitative Imaging in Medicine and Surgery, 13(2), 1164.

[16] Stephenson, N., Pushparajah, K., Wheeler, G., Deng, S., Schnabel, J. A., & Simpson, J. M. (2023). Extended reality for procedural planning and guidance in structural heart disease–a review of the state-of-the-art. The International Journal of Cardiovascular Imaging, 39(7), 1405-1419.

[17] Kong, B., Wang, X., Bai, J., et al. (2020). Learning tree-structured representation for 3D coronary artery segmentation. Computerized Medical Imaging and Graphics.

[18] Yang, X., Xu, L., Yu, S., Xia, Q., Li, H., & Zhang, S. (2024). Segmentation and vascular vectorization for coronary artery by geometry-based cascaded neural network. IEEE Transactions on Medical Imaging.

[19] Yang, Y. C., Dou, Y., Wang, Z. W., Yin, R. H., Pan, C. J., Duan, S. F., & Tang, X. Q. (2023). Prediction of myocardial ischemia in coronary heart disease patients using a CCTA–Based radiomic nomogram. Frontiers in Cardiovascular Medicine, 10, 1024773.

[20] Secinaro, A., Ntsinjana, H., Tann, O., Schuler, P. K., Muthurangu, V., Hughes, M., & Taylor, A. M. (2011). Cardiovascular magnetic resonance findings in repaired anomalous left coronary artery to pulmonary artery connection (ALCAPA). Journal of Cardiovascular Magnetic Resonance, 13, 1-6.

[21] Castaldi, B., Vida, V., Reffo, E., Padalino, M., Daniels, Q., Stellin, G., & Milanesi, O. (2017). Speckle tracking in ALCAPA patients after surgical repair as predictor of residual coronary disease. Pediatric cardiology, 38, 794-800.

[22] Krokovay, A., Pretre, R., Kretschmar, O., Knirsch, W., Valsangiacomo Buechel, E., & Dave, H. (2022). Anatomical reconstruction of proximal coronary artery stenosis in children. European Journal of Cardio-Thoracic Surgery, 62(3), ezac302.

[23] Jinmei, Z., Yunfei, L., Yue, W., & Yongjun, Q. (2020). Anomalous origin of the left coronary artery from the pulmonary artery (ALCAPA) is diagnosed in children and adolescents. Journal of cardiothoracic surgery, 15(1), 1-6.

[24] Zeng, A., Mi, C., Pan, D., Lu, Q., & Xu, X. (2022, December). ImageALCAPA: A 3D Computed Tomography Image Dataset for Automatic Segmentation of Anomalous Left Coronary Artery from Pulmonary Artery. In 2022 IEEE International Conference on Bioinformatics and Biomedicine (BIBM), IEEE, 1800-1803.